Modeling of Butadiene Polymerization Using Cobalt Octoate/DEAC/Water Catalyst

J. M. VELA ESTRADA, C. C. HSU, and D. W. BACON, *Chemical Engineering Department, Queen's University, Kingston, Ontario K7L 3N6, Canada*

Synopsis

Two-level fractional factorial designs were employed to study the solution polymerization of butadiene in a batch reactor using cobalt octoate/DEAC/water as catalyst. Conversion and molecular weight data obtained as functions of time were used to develop a kinetic model, and the estimated kinetic parameters were correlated empirically with four operating variables: temperature and concentrations of cobalt octoate, DEAC, and water. The experimental data indicate that at high water concentration a significant amount of oligomers is formed during early stages of polymerization, and the molecular weight of polymer increases with time. Analysis of the data suggests instantaneous initiation, first order propagation with cobalt and monomer, and transfer to monomer. Models which do not take account of the branching are shown to be incapable of fitting data for both $\overline{M}_n$ and $\overline{M}_w$. The catalyst decay seems to follow a first-order mechanism, but the evidence is somewhat inconclusive.

INTRODUCTION

Cis-polybutadiene can be prepared using Ziegler–Natta catalysts of titanium or cobalt compounds with aluminum alkyls. A cobalt catalyst usually has the advantage of high solubility in organic solvents and as a result is more efficient in terms of polymer yield per unit mass of catalyst used.

Several different cobalt salts have been reported to be effective for the 1,4-*cis* addition polymerization of butadiene, and cobalt salts of fatty acids have been used successfully in the commercial production of polybutadiene. The most common of these is cobalt octoate with diethyl aluminum chloride (DEAC) and water as cocatalysts. Despite its practical significance, however, the kinetics of this catalyst system have not been studied extensively.

Among the few publications on this subject appearing in the open literature is Gippin's[1] investigation of the kinetic behavior of cobalt octoate and the effects of water and its substitutes, such as cumene hydroperoxide, elemental bromine, and *tert*-butyl alcohol, on the activity of the catalyst and the quality of polymer produced after 19 h of reaction at 5°C. Gippin believed that part of the DEAC reacts with water or its substitutes to produce higher acid derivatives. A possible reaction of DEAC with those compounds is the dialkylation of DEAC by the substitution of a reactive electronegative group for one ethyl group.

Recently Honig et al.[2,3] reported kinetic data on butadiene polymerization with a cobalt octoate–DEAC catalyst. The results and the proposed mechanism formed the basis for a kinetic model developed by Hamielec and co-workers,[4] who used an empirical factor to take account of the efficiency of

Journal of Applied Polymer Science, Vol. 36, 655–673 (1988)
 CCC 0021-8995/88/030655-19$04.00

the cobalt catalyst. Their kinetic scheme assumes chain transfer to cobalt catalyst and butene-1 and a first-order deactivation of the catalyst. The concentrations of DEAC and water affect only the propagation rate constant, not the number of active sites. Based on those assumptions, their model correctly predicted trends in conversion and number average molecular weights, but the weight average molecular weight was consistently underestimated. The model could not fully account for the effect of water concentration.

In this work a batch reactor was used for polymerization. Under preselected operating conditions experiments were carried out according to two-level fractional factorial designs. The rate and average molecular weights were measured as functions of time to develop a kinetic model and estimate its kinetic parameters. The effects of temperature and concentration of DEAC, and of water, on those parameters were analyzed using empirical relationships. The kinetic model includes the branching reaction; without this reaction the model fails to predict both weight and number average molecular weights correctly.

EXPERIMENTAL

In this section a brief discussion of the experimental method is presented. Also discussed is the statistical experimental design strategy employed to acquire the necessary information to develop a comprehensive kinetic model.

Methods and Procedure

The reactor was a 1000 mL Pyrex kettle, equipped with the necessary reactant inlets and sampling and stirring devices. Temperature control was achieved by regulating the hot water flow rate through a heating coil inside the reactor while cold water was flowing through the reactor jacket at a constant rate. Both the hot and cold water temperatures were adjusted to achieve acceptable control so that the temperature could be easily maintained within $\pm 0.5°C$ of its target value.

The monomer, rubber grade butadiene with a purity of 99%, was obtained from Phillips Co. Butadiene was distilled out from the cylinder and passed through a series of drying columns containing drierite, type 4A molecular sieves and phosphorous pentoxide. The 25 wt % solution of DEAC in toluene was provided by Aldrich Chemical Co. and was used without further purification. ICN Pharmaceutical Inc. supplied the cobalt octoate, certified to contain 6 wt % cobalt; it was also used as received. The certified ACS analytical reagent grade toluene was dried by refluxing under a nitrogen atmosphere with sodium metal for at least 2 days. All operations were conducted under a dry nitrogen atmosphere.

In carrying out polymerization the reactor was assembled and flushed with dry nitrogen several times. Dry toluene was then added to the reactor followed by the butadiene solution. Fifty microliters of distilled water was added to the reactor. About 50 mL of the aliquot was withdrawn and analyzed for water content. More distilled water was then added to bring the total content to the desired level. DEAC was then added followed by the cobalt solution.

Sixteen samples were taken during each polymerization run at appropriate time intervals to determine monomer conversion and polymer molecular weights. The conversion was determined by a gravimetric technique, and a correction was applied to take account of the catalyst residues in the polymer samples. Gel permeation chromatography (GPC) was used for the determination of $\overline{M}_n$ and $\overline{M}_w$.

Data Collection

In a previous study,[5] we have shown that, for a polymerization system such as this one, data taken during early and late stages of polymerization runs contain most useful information for kinetic model building. Accordingly, the polymerization runs in this investigation were chosen to last for 3 h, at which time most of the polymerizations were expected to be complete. Sixteen samples were taken in each run, eight during the first hour, one during the second hour, and the rest during the last hour.

As mentioned earlier, two-level fractional factorial designs guided the selection of operating conditions; the conditions for the three sets of experimental runs are given in Table I. In designs 1 and 2 only conversion data were collected, and they were used to fit the conversion model. Design 2 differed

TABLE I
Operating Conditions for Polymerization Experiments[a]

Run code	Replicates	$[Al]_0$ (mmol/L)	$[Co]_0$ (mmol/L)	$[H_2O]_0$ (mmol/L)	T (°C)
		Design 1			
R-17	R1	30	0.10	9	30
R-14	R1, R2, R3	30	0.10	6	20
R-18	R1	30	0.05	9	20
R-11	R1	30	0.05	6	30
R-19	R1	20	0.10	9	20
R-10	R1	20	0.10	6	30
R-16	R1	20	0.05	9	30
R-15	R1	20	0.05	6	20
		Design 2			
R-7	R1, R2, R3	30	0.10	12	30
R-14	R1, R2, R3	30	0.10	6	20
R-13	R1	30	0.05	12	20
R-11	R1	30	0.05	6	30
R-12	R1, R2	20	0.10	12	20
R-10	R1	20	0.10	6	30
R-1	R1, R2, R3	20	0.05	12	30
R-15	R1	20	0.05	6	20
		Design 3			
R-12	R2	20	0.10	12	20
R-14	R2, R3	30	0.10	6	20
R-20	R1	20	0.10	6	20
R-21	R1	30	0.10	12	20

[a] For all experiments, $[M]_0 = 0.71$ mol/L.

from design 1 in the choice of the high level of water concentration. As will be discussed later, high water concentration changes the initial polymerization characteristics. Molecular weight data were obtained along with conversion data in design 3, in which only two variables, $[Al]_0$ and $[H_2O]_0$, were studied. According to our previous study,[5] the molecular weights are most influenced by these two variables.

Repeated runs were performed at selected operating conditions, and they are denoted by a suffix -R2, -R3, etc. Data from those replicates produced estimates of the pure error variance between runs and within runs. These error variance estimates are required to test for data heteroscedasticity, to assess the adequacy of the fitted models, and to evaluate the precision of the estimated model parameters.

Experimental Results

As Figure 1 shows, those runs with high water content (R-1-R1, -R2, -R3) exhibit a rapid increase in conversion during the first 5 min of polymerization but after that the conversion increases more slowly. The conversion curve behaves almost like a discontinuity at this transition. Since the conversion is

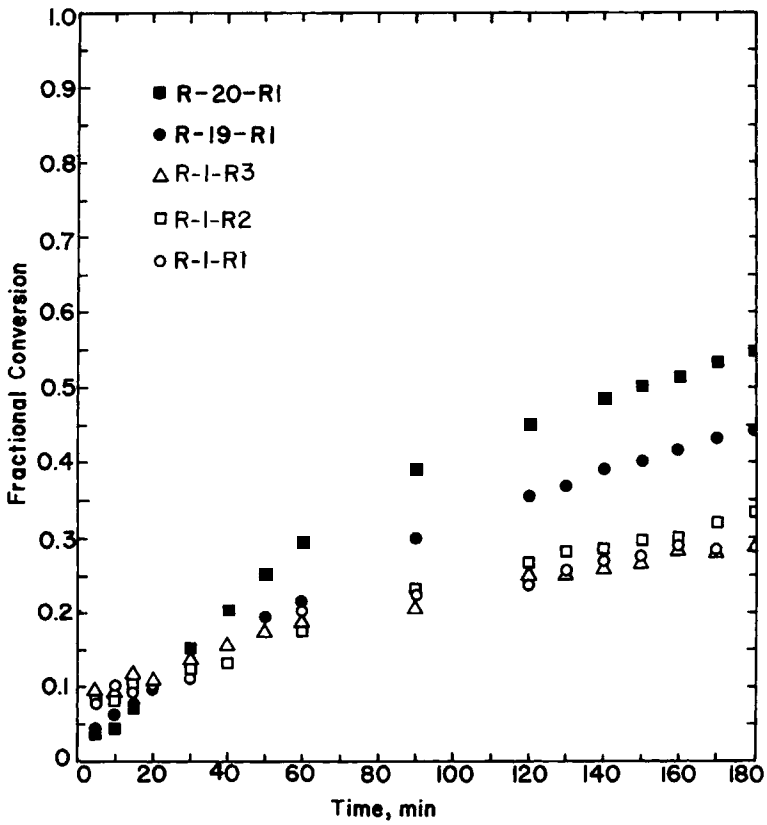

Fig. 1. Fractional conversion of butadiene as a function of time for polymerization runs R-20-R1 (■), R-19-R1 (●) and R-1-R1 (○), -R2 (□), -R3 (△). The experimental conditions are given in Table I. R-1-R1, -R2, -R3 are three replicate runs at operating conditions R-1.

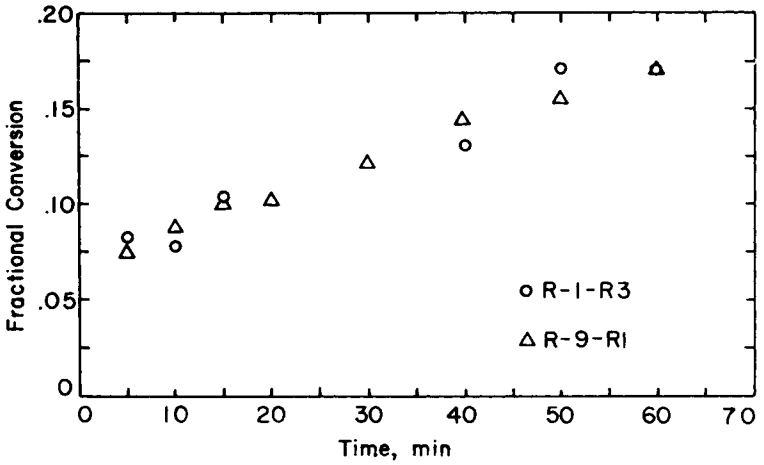

Fig. 2. A comparison of fractional conversions for two runs with different initial monomer concentrations. The initial monomer concentrations are 0.7 and 1.5 mol/L for runs R-1-R3 (○) and R-9-R1 (△), respectively.

low in this transition region and the amount of polymer in a sample is small, any inaccuracy in estimating the catalyst residues remaining in the sample could lead to a significantly large error in calculating conversion. To ensure that the rapid rise in conversion during the initial stage of polymerization was not caused by an error in estimating the catalyst residues, the experiment was repeated with twice the initial monomer concentration. With a first-order reaction with monomer, doubling the concentration of monomer should result in doubling the amount of polymer formed, while the fractional conversion remains the same. Thus, if the method of estimating the catalyst residues were inaccurate, two quite different fractional conversion curves would be expected since samples from these two runs should contain the same amounts of catalyst residues but different polymer contents. Figure 2 shows plots of fractional conversion vs. time for two experimental runs, one with an initial monomer concentration of 0.71 mol/L and another with 1.5 mol/L. The conversion curves for these two runs show no systematic deviation from each other. Thus, the sudden rise in conversion during the initial stage of polymerization reflects the true behavior of the system.

We are not aware of any previous reports of similar sudden rises in conversion during the initial stage of polymerization. In particular, Honig et al.[2,3] did not report any such jump in initial conversion. We believe that the reason for the difference between those results and ours is that Honig et al. used a lower water concentration (7.5 mmol/L) and a higher Al/H_2O ratio (3.3 or higher) for the polymerization, in contrast to a water concentration of 9 mmol/L or higher and an Al/H_2O ratio below 3.0 in this study for those experiments for which a conversion jump was observed. The high water concentration was deliberately chosen to facilitate the study of water effects.

Figure 1 also shows the degree of reproducibility of the data. The data points with different symbols for operating conditions R-1 represent three replicate runs (-R1, -R2, -R3). Conversion data for runs with lower water contents (R-19 and R-20) are included in Figure 1 for comparison. The

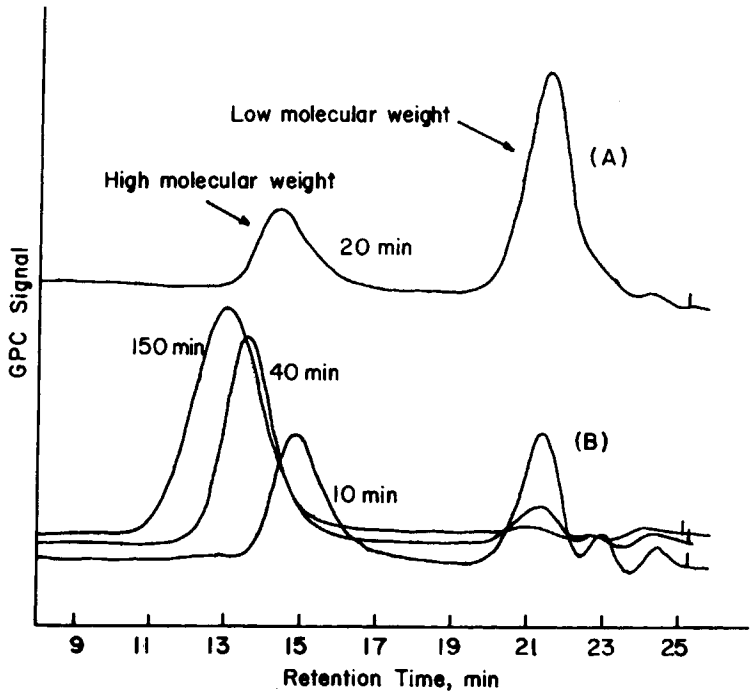

Fig. 3. GPC chromatograms of polymer samples (A) at 20 min during run R-12-R2 and (B) at 10, 40, and 150 min during run R-14-R2.

increase in conversion during the initial stage of polymerization is not as abrupt as in run R-1.

GPC chromatograms were obtained for all samples taken during the runs of design 3. Two sets of these chromatograms are shown in Figure 3. Curve A is from a sample taken after 20 min of polymerization during run R-12-R2, which had a water concentration of 12 mmol/L. The curves in set B are from samples taken at 10, 40, and 150 min of polymerization during run R-14-R2, which had a water concentration of 6 mmol/L. Two peaks were observed in all of these GPC curves. One appears in the region of high molecular weight (HMW) and the second in the region of very low molecular weight (LMW). The HMW peak covers the range of from 10,000 to 260,000 in M_w. Since the LMW peak shows an M_w below the lowest molecular weight of the standard polybutadiene samples normally available, we are uncertain about its range of molecular weight; however, it is reasonable to believe that the LMW materials are oligomers probably formed during the very early stage of polymerization.

It is interesting to note that while the LMW peak appears almost at the onset of the polymerization, the HMW peak is hardly noticeable in the chromatograms taken during the first few minutes of polymerization, but grows in size and shifts to higher molecular weights with time. The retention times, or elution volumes (the GPC was run at a flow rate of 1 mL/min) of the LMW peaks for samples taken at different times, are fairly consistent, but the size for the high water run R-12-R2 is much larger than for the low water run

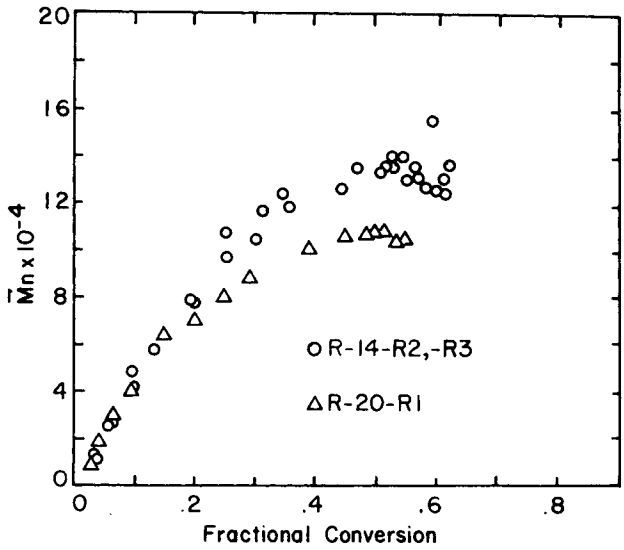

Fig. 4. A plot of number average molecular weight as a function of fractional conversion. $[Al]_0$ = 30 mmol/L for runs R-14-R2 and -R3 and 20 mmol/L for run R-20-R1. Other conditions are given in Table I.

(R-14-R2). The size of LMW peak also decreases with time; this should not be misunderstood as a decrease of the amount of oligomers formed. The sample volume used for the GPC analyses was adjusted so that the weight percent of polymer in the sample remained approximately the same. Thus the polymer sample size used in preparing the solution for GPC analysis was decreased accordingly as conversion increased, which resulted in a decreasing amount of oligomers in samples injected into the GPC.

Comparing the conversion curves and GPC results at different water concentation levels, one can conclude that high water concentration is responsible for the formation of oligomers. The oligomers must be formed during a very early stage of polymerization; this is shown in the conversion plot where a "jump" in conversion is observed for high water runs. When the water level is low, the oligomer peak can still be noticed, but its size was much smaller and the conversion curve is not characterized by a "jump" at low conversion.

Figures 4 and 5 show some results for $\bar{M}_n$ as a function of conversion. Clearly, the molecular weight increases with conversion. In comparing two runs with high (30 mmol/L) and low (20 mmol/L) alkyl concentrations (Fig. 4), the two $\bar{M}_n$ curves overlap in the low conversion region, but they deviate at high conversions where higher $\bar{M}_n$ is obtained at the higher aluminum level. Figure 5 is a comparison of $\bar{M}_n$ for two different water levels. At low conversion the lower $\bar{M}_n$ at higher water level should not be interpreted as a direct effect of water on molecular weight. With a water concentration of 12 mmol/L, a significant amount of oligomers was formed; thus a higher proportion of monomer that reacted formed oligomers. If this is taken into consideration, water should have little effect on molecular weight as is shown to be the

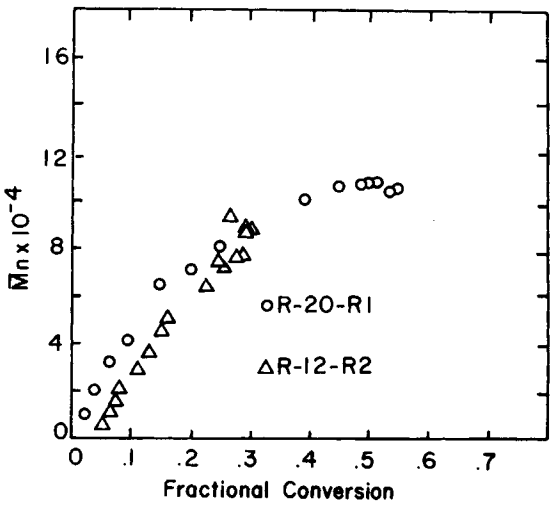

Fig. 5. A plot of number average molecular weight as a function of fractional conversion. $[H_2O]_0$ = 6 mmol/L for run R-20-R1 and 20 mmol/L for run R-12-R2. Other conditions are given in Table I.

case at the higher conversions. Therefore, transfer reactions to aluminum alkyl and water or water-related compounds are not likely.

Honig et al.[3,4] suggested that the transfer reaction is the result of the detachment of polymer molecules from active cobalt complexes, leaving the complexes still active for further chain growth. No real evidence was presented to substantiate such a mechanism. We believe that this type of reaction is possible only in the presence of monomer. Therefore, our model assumes a transfer reaction to monomer.

Model Development

Two different mechanisms can be postulated to describe the phenomena observed in these experiments:

1. As a result of fast initiation, highly active complexes are formed almost instantaneously, and the monomer is polymerized at a very fast rate. However, an excess amount of water in the reaction mixture acts as a chain termination agent and deactivates the catalyst quickly until all water is consumed. The rapid deactivation is responsible for the formation of oligomers. The remaining complexes, in greatly reduced concentrations, polymerize the monomer at a much slower overall polymerization rate. The complexes which survive the initial deactivation are still subjected to a chain termination reaction, but probably by a different mechanism.

2. The initiation reaction may produce two different species of active complexes, a stable one that is responsible for the formation of long chains and an unstable one that produces oligomers.

To discriminate between these two models would require substantial experimental data during the first 5 min of polymerization. Unfortunately, this was not possible with the apparatus we used. In fact, it would be extremely difficult to design an apparatus that could produce enough molecular weight

data as well as conversion data during the initial stage of polymerization to allow a detailed comparison of these two mechanisms.

After the formation of oligomers or the completion of the first stage deactivation reaction, there is no distinction between these two models. For this reason and in light of the experimental constraints described above, the model developed here covers only the period starting from the end of first stage deactivation as characterized by a time parameter t_0.

The underlying assumptions made in the development of the model are: (1) instantaneous initiation; (2) first-order propagation with monomer; (3) chain transfer to monomer; (4) branching reaction due to 1,2 vinyl polymerization; and (5) first-order termination. The assumption of an instantaneous initiation reaction is based on the absence of an induction period. The overlap of fractional conversion curves with different monomer concentrations under the same polymerization conditions as shown in Figure 2 is an indication of first-order polymerization with respect to monomer as generally believed. The transfer reaction to monomer, as discussed earlier, is plausible. Justification of the other assumptions will be discussed later.

With these assumptions, the polymerization reactions can be written as follows:

(i)	$C_0 + DEAC + H_2O \longrightarrow I^*$	instantaneous complex formation
(ii)	$I^* + M \longrightarrow P_1$	instantaneous initiation
(iii)	$P_r + M \xrightarrow{k_p} P_{r+1}$	propagation
(iv)	$P_r + M \xrightarrow{k_{tm}} Q_r + I^*$	transfer to monomer
(v)	$P_r + Q_s \xrightarrow{k_{br}} P_{r+s}$	branching
(vi)	$P_r \xrightarrow{k_d} Q_r$	deactivation

where the k's are the rate constants and M, P_r, and Q_r are, respectively, the monomer, active polymer with chain length r, and dead polymer with chain length r. The rate equations can then be written accordingly:

$$\frac{d[M]}{dt} = -k_{tm}[M]L_0 - k_p[M]L_0 \tag{1}$$

$$\frac{d[P_1]}{dt} = -(k_p[M] + k_d + k_{tm}[M])[P_1] + k_{tm}[M]L_0 - k_{br}[P_1]J_0 \tag{2}$$

$$\frac{d[P_r]}{dt} = -k_p[M]([P_r] - [P_{r-1}]) - (k_d + k_{tm}[M] + k_{br}J_0)[P_r] + k_{br}\sum_{s=1}^{r-1}[P_{r-s}][Q_s] \qquad \text{for } r > 1 \tag{3}$$

$$\frac{d[Q_r]}{dt} = k_d[P_r] + k_{tm}[M][P_r] - k_{br}[Q_r]L_0 \tag{4}$$

where J_n and L_n are moments of nth order, defined as

$$J_n = \sum_{r=1}^{\infty} r^n[Q_r] \quad \text{and} \quad L_n = \sum_{r=1}^{\infty} r^n[P_r] \tag{5}$$

The initial conditions can be summarized as follows:

$$\text{at } t = 0,\ [M] = [M]_0,\ [A1] = [A1]_0,$$

$$[P_r] = [Q_r] = J_n = 0$$

$$[P_1] = L_n = [I^*]_0$$

In formulating eqs. (1)–(4), we assume negligible volume change due to polymerization.

Multiplying eqs. (3) and (4) with r^0, r^1, and r^2 and summing over all values of r, we obtain the following moment equations:

$$\frac{dL_0}{dt} = -k_d L_0 \tag{6}$$

$$\frac{dL_1}{dt} = (k_p + k_{tm})[M]L_0 - (k_d + k_{tm}[M])L_1 + k_{br}L_0J_1 \tag{7}$$

$$\frac{dL_2}{dt} = 2k_p[M]L_1 + (k_p + k_{tm})[M]L_0 - (k_d + k_{tm}[M])L_2 + k_{br}(L_0J_2 + 2L_1J_1) \tag{8}$$

$$\frac{dJ_0}{dt} = (k_{tm}[M] + k_d)L_0 - k_{br}L_0J_0 \tag{9}$$

$$\frac{dJ_1}{dt} = (k_{tm}[M] + k_d)L_1 - k_{br}L_0J_1 \tag{10}$$

$$\frac{dJ_2}{dt} = (k_{tm}[M] + k_d)L_2 - k_{br}L_0J_2 \tag{11}$$

Equations (1) and (6) can be solved separately to give the conversion model:

$$-\ln\left[\frac{[M]}{[M]_0}\right] = -\ln\left[\frac{[M]_{t_0}}{[M]_0}\right] + \left[\frac{k_p[I^*]_{t_0}}{k_d}\right] \times \{1 - \exp[k_d(t_0 - t)]\} \tag{12}$$

where t_0 is the polymerization time at which the formation of oligomers is complete. Unfortunately, t_0 cannot be determined experimentally; it is treated

here as another parameter. Defining the lumped parameters as

$$\theta_1 = -\ln([\mathrm{M}]_{t_0}/[\mathrm{M}]_0)$$

$$\theta_2 = k_p[\mathrm{I}^*]_{t_0}$$

Eq. (12) becomes

$$-\ln\left[\frac{[\mathrm{M}]}{[\mathrm{M}]_0}\right] = \theta_1 + \left[\frac{\theta_2}{k_d}\right]\{1 - \exp[-k_d(t - t_0)]\} \tag{13}$$

Equations (7)–(11) must be integrated numerically to obtain the first and second moments of L and J. The number and weight average molecular weights can then be calculated by

$$\overline{M}_n = \frac{L_1 + J_1}{L_0 + J_0} M_m \tag{14}$$

$$\overline{M}_w = \frac{L_2 + J_2}{L_1 + J_1} M_m \tag{15}$$

where M_m is the molecular weight of the monomer.

Parameter Estimation

Parameters θ_1, θ_2, k_d, and T_0 were estimated by fitting the conversion model given in eq. (13) to each experimental run in designs 1 and 2. Empirical relationships were then developed between these estimates and the operating conditions. For design 3, where $\overline{M}_n$ and $\overline{M}_w$ as well as conversion were measured, the above parameters plus k_{tm} and k_{br} were estimated by fitting all three models [eqs. (13)–(15)] simultaneously to the data for the three response variables.

Ordinary least squares was employed to fit eq. (13) to the measured conversion data for each run. For those operating conditions at which replicate runs were conducted, all the replicates were lumped together to estimate the parameters for that particular set of operating conditions. Vela Estrada[6] has provided a detailed description of the estimation procedure. The parameter estimates obtained for eq. (13) are shown in Table II.

For solving the moment equation, eqs. (7)–(11), a robust subroutine is required because of the variation in the stiffness of the differential equations with various parameter values tested in searching for an optimum fit. A routine called SECDER developed at the University of Toronto[7,8] based on Enright's second derivative formulae[7] was found to be efficient for this purpose. The Box–Draper criterion,[9] which minimizes the determinant of the matrix of sums of squares and cross products of the residuals of the responses, was used to fit models (13), (14), and (15) simultaneously to the data for conversion, $\overline{M}_n$ and $\overline{M}_w$ from design 3. The resulting of parameter estimates for each run in design 3 are presented in Table III.

TABLE II
Parameter Estimates for Conversion Model [eq. (13)] for the 14 Sets of Operating Conditions in Designs 1, 2, and 3[a]

Expt. run	t_0 (min)	θ_1 (min^{-1})	θ_2 (min^{-1})	k_d (min^{-1})
R-1-R1, -R2, -R3	5	0.0854	0.0021	0.0033
		(0.0087)	(0.0002)	(0.0013)
R-7-R1, -R2, -R3	5	0.0553	0.0067	0.0062
		(0.0153)	(0.0005)	(0.0012)
R-10-R1	0	—	0.0124	0.0094
			(0.0001)	(0.0002)
R-11-R1	5	0.0382	0.0059	0.0074
		(0.0023)	(0.0001)	(0.0003)
R-12-R1, -R2	5	0.0559	0.0028	0.0047
		(0.0102)	(0.0003)	(0.0014)
R-13-R1	5	0.0527	0.0021	0.0049
		(0.0087)	(0.0002)	(0.0016)
R-14-R1, -R2, -R3	0	—	0.0083	0.0049
			(0.0002)	(0.0004)
R-15-R1	5	0.0231	0.0031	0.0043
		(0.0047)	(0.0001)	(0.0005)
R-16-R1	5	0.0431	0.0049	0.0068
		(0.0028)	(0.0001)	(0.0003)
R-17-R1	0	—	0.0155	0.0114
			(0.0001)	(0.0002)
R-18-R1	5	0.0487	0.0024	0.0025
		(0.0036)	(0.0001)	(0.0004)
R-19-R1	5	0.00395	0.0042	0.0036
		(0.0036)	(0.0001)	(0.0003)
R-20-R1	0	—	0.0061	0.0038
			(0.0001)	(0.0005)
R-21-R1	5	0.0432	0.0041	0.0058
		(0.0027)	(0.0001)	(0.0003)

[a] Note: The value in parentheses is the standard deviation associated with corresponding estimate.

TABLE III
Parameter Estimates for the Multiresponse Model for Conversion, $\overline{M}_n$ and $\overline{M}_w$ Fitted to Each Experimental Run of Design 3

Expt. run	$[I^*]_{t_0} \times 10^4$ (mol/L)	k_p (L/mol min)	$k_{tm} \times 10^2$ (L/mol min)	k_{br} (L/mol min)	$k_d \times 10^3$ (min^{-1})
R-12-R2[a]	0.256	109.4	8.35	254.1	6.09
			(1.25)	(42.4)	(0.70)
R-14-R2, -R3	0.467	178.5	5.69	31.8	5.28
	(0.020)	(5.5)	(0.34)	(5.6)	(0.36)
R-20-R1	0.381	159.4	8.16	120.5	3.69
	(0.034)	(14.2)	(1.15)	(18.6)	(0.51)
R-21-R1[a]	0.368	109.9	6.51	102.0	58.3
			(0.66)	(17.8)	(0.3)

[a] Before the model was fitted to the molecular weight data values of k_d and the lumped parameter $k_p[I^*]_{t_0}$ obtained from Table II, where the conversion model alone was fitted to the data, were substituted into the molecular weight model. However, wherever the concentration of active sites, $[I^*]_{t_0}$, appears separately from k_p in the moecular weight model, it was treated as a separated parameter and was estimated. The estimate of k_p was then calculated from $k_p[I^*]_{t_0}/[I^*]_{t_0}$. The value in parentheses is the standard deviation associated with the estimate.

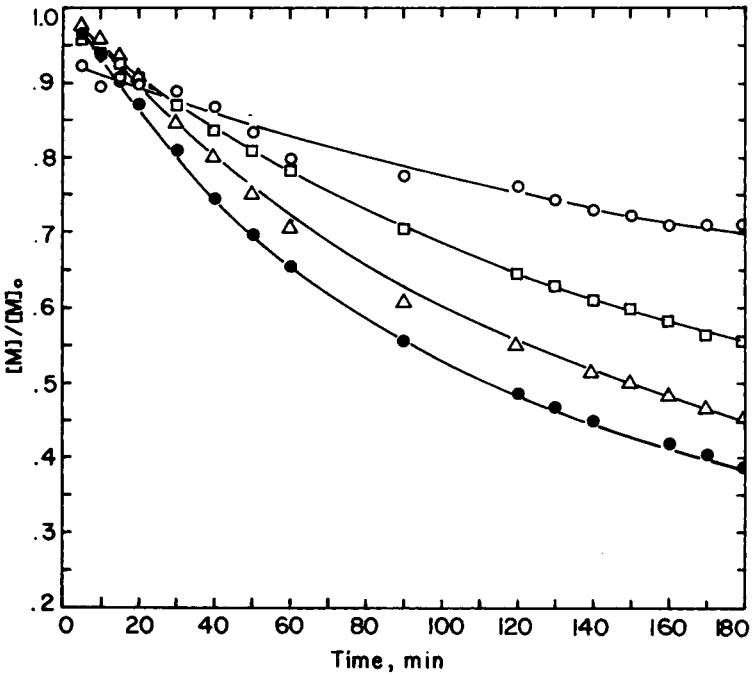

Fig. 6. Comparisons of model predicitions of $[M]/[M]_0$ and experimental data. Polymerization conditions are given in Table I: (○) R-1-R2; (□) R-19-R1; (△) R-20-R1; (●) R-14-R2.

In order to test the adequacy of a fitted model and calculate the precision of its parameter estimated, it is necessary to know the pure error variance. Bartlett's test[10] for heteroscadasticity was applied to those experimental conditions where replicate runs were available, R-1, R-7, R-12, and R-14. The results showed no significant difference in variance among conditions R-1, R-12, and R-14, but the variance for condition R-7 was clearly different for no apparent reason. Pooling the three variances from conditions R-1, R-12, and R-14 provided an overall estimate of pure error variance of 0.0003115. This value was used as an estimate of the pure variance for single experimental runs.

The adequacy of the model was assessed using an F-test and residuals plots from the fitted model[11]. The fitted model for each of the 14 sets of operating conditions passed the F-test. However, for the replicate set R-14 and run R-20-R1 the confidence intervals for the estimate of θ_1 included only negative values. Furthermore, the residuals plots for those runs showed trends with time. When θ_1 was given a value of zero for those runs to make it physically meaningful, trends in the residuals plots remained even though the fitted model still passed the F-test. There is no apparent explanation for these residuals trends.

With the two exceptions mentioned above, it can be concluded that the proposed model provides an adequate representation of the data in the experimental region studied. For illustration, Figure 6 shows a comparison of experimental and predicted values of $[M]/[M]_0$ vs. time for runs R-1-R1,

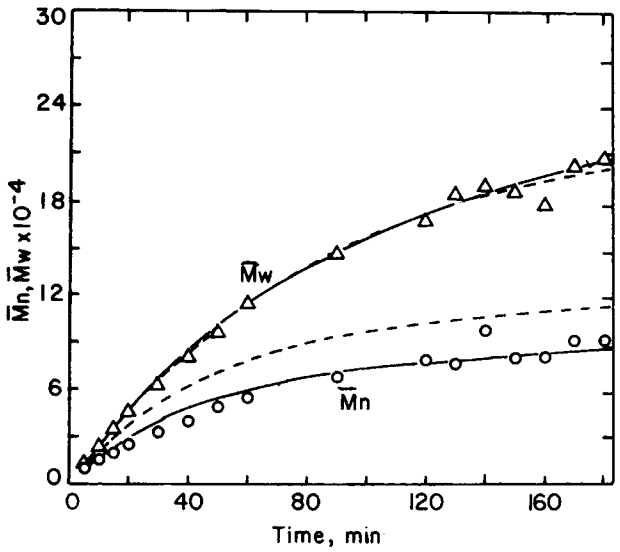

Fig. 7. Comparisons of predicted values of $\bar{M}_n$ and $\bar{M}_w$ with experimental data for run R-12-R2: (—) calculated from the model including the branching reaction; (- - -) calculated by ignoring branching.

R-14-R2, R-19-R1, and R-20-R1. Run R-20-R1 is one exhibiting a trend in the residuals plot. Predicted values for $\bar{M}_n$ and $\bar{M}_w$ are illustrated in Figure 7 for run R-12-R2.

RESULTS AND DISCUSSION

Conversion Model

As pointed out in the previous section, the conversion model, eq. (13), appears to represent the data adequately. This model assumes a first-order deactivation of catalyst. However, Zgonnik and co-workers[12] have suggested a second-order deactivation for $CoCl_2 \cdot 2Py$–DEAC catalyst system. Second-order deactivation has also been reported for $Co(acac)_3$–DEAC catalyst by Bawn[13] and Yang and Hsu.[14] For this reason a model with second-order deactivation was derived and fitted to the conversion data from designs 1 and 2.

It has already been demonstrated that the model with first-order deactivation is adequate in representing the data in the experimental region defined by designs 1, 2, and 3. No inadequacy was found in the fitted model with second-order deactivation using an F-test at each set of operating conditions, but the residuals plots for the runs with water concentration at 6 and 9 mmol/L levels showed clear trends with time. With the exception of two conditions, R-14 and R-20, the residual plots for first-order model show no trends at those water levels. Also, the likelihood ratio for these two fitted models, defined as the ratio of the maximum likelihood of the first-order deactivation model to the maximum likelihood of second-order deactivation

model, yielded values of 5.98, 8.06, and 5.6 for conditions R-10, R-14, and R-17, respectively, while the ratios for the other conditions were close to 1.0. A large likelihood ratio would favor a first-order deactivation. Three out of the 14 sets of conditions fall into that category.

Thus, the evidence apparently favors a first-order deactivation model, but cannot be considered conclusive. However, for the purpose of providing an acceptable kinetic model, it appears reasonable.

The estimated values of the kinetic parameters under different operating conditions are given in Tables II and III. Since no experimental data are available below 5 min reaction time, it is not possible to obtain an estimate of the parameter t_0 between 0 and 5 min. With t_0 equal to zero, $\theta_1 (= -\ln [M]_{t_0}/[M]_0)$ will also be zero by definition. With the exception of condition R-17 where $[H_2O]_0 = 9$ mmol/L, all low water level runs give a zero value for t_0. On the other hand, when the water level is high, the model fits well with $t_0 = 5$ min. Under no circumstance was an estimate of t_0 greater than the 5 min obtained. The monomer conversions at $t = t_0$, calculated from the estimates of θ_1, vary from 0 (at $\theta_1 = 0$) to about 8% ($\theta_1 = 0.0854$).

Since exact knowledge of the functional relationships between the kinetic parameters and the operating variables was not available, we developed them empirically using first-order relationships. From regression analysis, retaining only significant terms, we obtained the following relationships for the parameter $k_p[I^*]_{t_0}$ for designs 1 and 2, respectively:

$$10 \ln\left(k_p[I^*]_{t_0}\right) = -51.37 + 0.96[Al]'_0 + 4.26[Co]'_0 - 1.08[H_2O]'_0 + 3.86T' + 1.19[Al]'_0[Co]'_0 \quad (16)$$

$$10 \ln\left(k_p[I^*]_{t_0}\right) = -54.31 + 1.55[Al]'_0 + 4.01[Co]'_0 - 3.83[H_2O]'_0 + 2.46T' \quad (17)$$

where the superscript $'$ denotes a coded value of the operating variable defined by

$$\text{coded value} = \frac{\text{measured value} - (1/2)(\text{upper limit} + \text{lower limit})}{(1/2)(\text{upper limit} - \text{lower limit})} \quad (18)$$

where the values of the lower and upper limits can be found in Table I. For example, for design 1 the lower and upper limits of $[Al]_0$ are 20 and 30 mmol/L, respectively.

The coefficients reflect the individual effects of the corresponding operating variables and their interaction effects with other operating variables. Equations (16) and (17) show that, as expected, all four operating variables are important in explaining changes in the parameter $k_p[I^*]_{t_0}$ with operating conditions. Water is the only variable that has a negative coefficient on activity. However, it should be pointed out that the equation applies only to the range of conditions studied. If the water content were reduced to a

minimal value, we would expect a positive water effect on polymerization, since it has been shown by Gippin[1] that polymerization cannot be initiated without the presence of water in trace amounts.

The interaction effect between $[Al]_0$ and $[Co]_0$ was found to be important for the range of water concentration from 6 to 9 mmol/L (design 1), while this effect was unimportant for a water concentration range from 6 to 12 mmol/L (design 2). This result is somewhat surprising, and we cannot offer an explanation. Normally the smaller the range of an operating variable, the smaller the interaction effects are expected to be.

We now consider the activity parameter, $k_p[I^*]_{t_0}$, in another form. It is not unreasonable to express $k_p[I^*]_{t_0}$ in the form

$$k_p[I^*]_{t_0} = \alpha[Al]_0^a \cdot [H_2O]_0^b[Co]_0^c \exp(-E/RT) \tag{19}$$

where α, a, b, and c are constants, E the activation energy for the propagation reaction, and R the gas constant. Taking logarithms of both sides of eq. (19) produces a first-order model. Using that model, estimates of $\ln \alpha$, a, b, c, and E were obtained by linear regression using the estimates of $k_p[I^*]_{t_0}$ for each run of design 2. The resulting parameter estimates are 18.3(3.1), 0.77(0.22), −1.10(0.12), 1.15(0.13), and 2.1(0.4) (E in kJ/mol), respectively. The value shown in parentheses is the standard deviation.

The activation energy obtained here is very close to values reported for polymerizations of butadiene with other cobalt based catalysts. Zgonnik et al.[15] obtained an E value of 1.7 kJ/mol using $CoCl_2 \cdot 2Py$ while Ho et al.[16] obtained a value of 2.1(0.3) kJ/mol using $CoCl_2 \cdot 4Py$. Perhaps more importantly, the regression analysis [eq. (19)] produced a low correlation (0.318) between the activation energy and the coefficient for the water term. This seems to suggest that water only affects the number of active centers but not the activity or k_p, contrary to Honig et al.[2,3]

The relationships between k_d and the operating variables were obtained in a similar fashion for designs 1 and 2, respectively, as follows:

$$\begin{aligned} 10 \ln k_d = &-51.77 + 1.53[Co]_0' - 0.88[H_2O]_0' + 4.17T' \\ &+ 1.16[H_2O]_0'T' + 0.65[Co]_0'[H_2O]_0' \end{aligned} \tag{20}$$

$$10 \ln k_d = -52.38 \tag{21}$$

For design 1 the effect of aluminum was found to be negligible. Water shows a negative effects on k_d, but interestingly both interaction effects of water with temperature and cobalt concentration are important and positive. As the range of water increases from 6–9 to 6–12 mmol/L, k_d becomes independent of all four operating variables. This suggests that for a wide range of water concentration the effect of water on the termination reaction is much more complicated than a simple linear correlation can represent. On the other hand, a relationship was obtained from the results of design 1 because a complex process can often be approximated by a simple linear equation when the range of representation is not too large. The termination step is often further complicated by the possible presence of traces of unknown impurities.

Molecular Weight Models

As mentioned previously, the molecular weight model was fitted to the data obtained using design 3 for conversion, $\overline{M}_n$ and $\overline{M}_w$ simultaneously. The k_d estimates obtained for the four conditions tested in design 3 agree well with those for the corresponding conditions given in Table II. The latter estimates were obtained from monomer conversion only. This is an encouraging indication of the validity of the model.

A comparison of predicted values of $\overline{M}_n$ and $\overline{M}_w$ from the fitted models with experimental data is shown in Figure 7. This figure also includes plots (shown by dotted lines) of $\overline{M}_n$ and $\overline{M}_w$ for the models in which the branching reaction is absent. The estimated values of $\overline{M}_w$ without considering branching agrees well with the experimental data, but this is not the case for $\overline{M}_n$. That model also failed the F-test, and the residuals plots showed clear trends with time in all runs. In addition, the polydispersity predictions were consistently below the experimental values. Similar results were obtained by Honig et al.[4] from a model in which branching was also ignored.

The underestimation of polydispersity clearly suggests the possibilities of large molecules forming due to transfer to dead polymer or of branching (termination by combination is unlikely, as discussed before), neither of which is accounted for in this simplified model. However, inclusion of the transfer reaction to dead polymer alone did not improve the model; in fact, the estimates of the transfer rate constant were negative.

On the other hand, including the branching reaction [reaction (v) of the kinetic scheme] produced good agreement between predicted and experimental values of both $\overline{M}_n$ and $\overline{M}_w$, as shown by the solid lines in Figure 7. However, for the replicate set R-14 and run R-20-R1 the fitted molecular weight models failed the F-test. These two sets of experimental data also produced trends in the residuals plots when the conversion model was fitted to the data.

The possibility of branching for polybutadiene synthesized with $CoCl_2$–Al $(i-Bu)_2Cl$ catalyst has also been discussed by Poddubnyi et al.[17] They obtained a polydispersity of 2.19. The polydispersity found in this investigation varied from about 1.6 to 2.5. Yang and Hsu[14] observed very high polydispersity, up to 7.0, for $Co(acac)_3$ catalyst. The polymer produced by their catalyst contained about 40% vinyl structure. Therefore, it is likely that the branching reaction originated from a 1,2 vinyl polymerization, which creates a branch chain with unsaturated vinyl structure. The dead polymer with such a side chain may in turn react with a growing chain to form long branching. Likely, the following reactions leading to branching are possible:

1,2 polymerization:

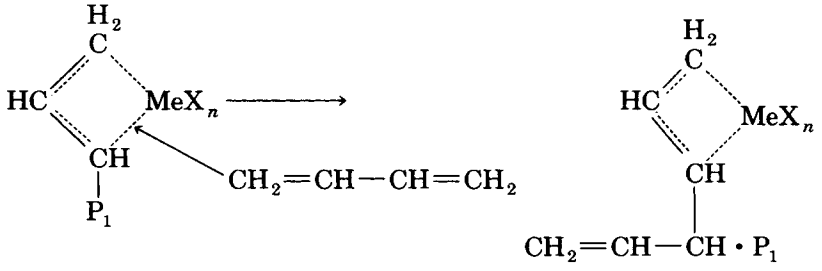

Branching reaction:

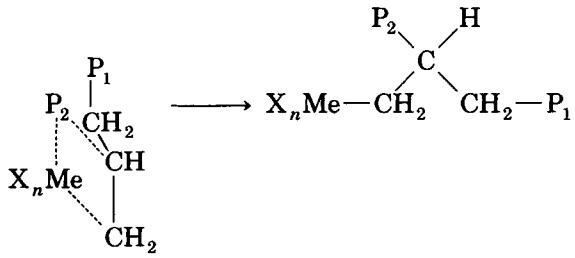

The values of the rate constant for the branching reaction k_{br} given in Table III may serve as a measure of degree of branching. k_{br} increases with an increase in water concentration. Table III also provides estimates of the number of active centers $[I^*]_{t_0}$. The value varies with water concentration as well, in accord with the results of the analysis of the parameter $k_p[I^*]_{t_0}$ from the conversion data.

CONCLUSION

A kinetic model for butadiene polymerization over cobalt octoate/DEAC/H_2O catalyst was developed based on experimental conversion and molecular weight data. The study shows that the initiation reaction is instantaneous, the propagation follows a first-order reaction with cobalt and monomer, and the chain growth is terminated by either transfer to monomer or catalyst deactivation. The latter seems to follow a first-order reaction, but the evidence is not conclusive. The branching reaction was found to be important and must be included in the model in order to predict both $\bar{M}_n$ and $\bar{M}_w$ correctly.

Water plays a very significant role in the polymerization. The catalyst activity is enhanced by the presence of water, but if water is present in excess, a significant amount of oligomers is formed during the very early stage of polymerization. Water is also involved in catalyst deactivation.

Experimental design techniques and statistical analysis were employed throughout this investigation. It has been demonstrated that they are effective in providing the necessary information with minimal experimental effort.

This research was funded by the Natural Sciences and Engineering Research Council of Canada. Funds from Consejo Nacional de Ciencia y Tecnologia, Mexico City, Mexico and Universidad Autonomade Nuevol Leon, Monterrey, Mexico supported J. M. Vela Estrada during his stay at Queen's University.

References

1. M. Gippin, *Ind. Eng. Chem. Prod. Res. Dev.*, **4**, 160 (1965).
2. J. A. J. Honig, R. P. Burford, and R. P. Chaplin, *J. Polym. Sci., Polym. Chem. Ed.*, **21**, 2559 (1983).
3. J. A. J. Honig, R. P. Burford, and R. P. Chaplin, *J. Polym. Sci., Polym. Chem. Ed.*, **22**, 1461 (1984).
4. J. A. J. Honig, P. E. Gloor, J. F. MacGregor, and A. E. Hamielec, *J. Appl. Polym. Sci.*, **34**, 829 (1987).
5. J. M. Vela Estrada, C. C. Hsu, and D. W. Bacon, *Polym. Plast. Technol. Eng.*, to appear.

6. J. M. Vela Estrada, Ph.D. thesis, Chem. Eng. Dept., Queen's Univ., Kingston, ON, Canada, 1986.

7. W. Enright, "Studies in the Numerical Solution of Stiff Ordinary Differential Equations," Technical Report No. 46, Dept. of Comput. Sci., Univ. of Toronto, Toronto, ON, Canada, 1972.

8. C. A. Addison, "Implementing a Stiff Method Based upon the Second Derivative Formulas," Technical Report No. 139, Dept. of Comput. Sci., Univ. of Toronto, Toronto, ON, Canada, 1979.

9. G. E. P. Box and N. R. Draper, *Biometrika*, **52**, 355 (1965).

10. M. S. Bartlett, *Proc. Roy. Soc. A*, **160**, 268 (1937).

11. N. R. Draper and H. Smith, *Applied Regression Analysis*, Wiley, New York, 1980.

12. V. N. Zgonnik, B. A. Dolgoplosk, N. I. Nikolayev, and V. A. Koprachev, *Polym. Sci. U.S.S.R.*, 4(7), 1000 (1962).

13. C. E. H. Bawn, *Rubber Plast. Age*, **46**, 510 (1965).

14. W. L. Yang and C. C. Hsu, *J. Appl. Polym. Sci.*, **28**, 145 (1983).

15. V. N. Zgonnik, B. A. Dolgoplosk, N. I. Nikolayev, and V. A. Kropachev, *Polym. Sci. U.S.S.R.*, 7(2), 308 (1965).

16. F. K. W. Ho, C. C. Hsu, and D. W. Bacon, *J. Appl Polym. Sci.*, **32**, 5287 (1986).

17. I. Ja. Poddubnyi, V. A. Grechanovskii, and E. G. Ehrenburg, *Makromol, Chem.*, **94**, 268 (1966).

Received August 17, 1987
Accepted October 16, 1987